

High speed hybrid silicon evanescent Mach-Zehnder modulator and switch

Hui-Wen Chen, Ying-hao Kuo, and John E. Bowers

*Department of Electrical and Computer Engineering,
University of California Santa Barbara,
Santa Barbara, CA 93106
hwchen@ece.ucsb.edu*

Abstract: We demonstrate the first high speed silicon evanescent Mach Zehnder modulator and switch. The modulator utilizes carrier depletion within AlGaInAs quantum wells to obtain $V_{\pi}L$ of 2 V-mm and clear open eye at 10 Gb/s. The switch exhibits a power penalty of 0.5 dB for all ports at 10 Gb/s modulation.

©2008 Optical Society of America

OCIS codes: (250.4410) Modulators; (250.5300) Photonic integrated circuits; (250.7360) Waveguide modulators.

References and Links

1. A. S. Liu, R. Jones, L. Liao, D. Samara-Rubio, D. Rubin, O. Cohen, R. Nicolaescu, and M. Paniccia, "A high-speed silicon optical modulator based on a metal-oxide semiconductor capacitor," *Nature* **427**, 615–618 (2004).
2. D. Marris-Morini, X. Le Roux, L. Vivien, E. Cassan, D. Pascal, M. Halbwax, S. Maine, S. Laval, J. M. Fedeli, and J. F. Damlencourt, "Optical modulation by carrier depletion in a silicon PIN diode," *Opt. Express* **14**, 10838-10843 (2006).
3. Q. Xu, S. Pradhan, B. Schmidt, J. Shakya, and M. Lipson, "12.5 Gbit/s carrier-injection-based silicon micro-ring silicon modulators," *Nature* **435**, 325-327 (2005).
4. Y.-H. Kuo, H.-W. Chen, and J. E. Bowers, "High speed hybrid silicon evanescent electroabsorption modulator," *Opt. Express* **16**, 9936-9942 (2008).
5. H.-W. Chen, Y.-H. Kuo, and J. E. Bowers, "A Hybrid Silicon-AlGaInAs Phase Modulator," *IEEE Photon. Technol. Lett.* **23** (to be published)
6. A. W. Fang, E. Lively, Y.-H. Kuo, D. Liang, and J. E. Bowers, "A distributed feedback silicon evanescent laser," *Opt. Express* **16**, 4413-4419 (2008).
7. H. Park, Y.-h Kuo, A. W. Fang, R. Jones, O. Cohen, M. J. Paniccia, and J. E. Bowers, "A hybrid AlGaInAs-silicon evanescent preamplifier and photodetector," *Opt. Express* **15**, 13539-13546 (2007).
8. H. Ohe, H. Shimizu, and Y. Nakano, "InGaAlAs Multiple-Quantum-Well Optical Phase Modulators Based on Carrier Depletion," *IEEE Photon. Technol. Lett.*, **19**, 1616-1618 (2007).
9. D. Liang, E. A. Lucero, and J. E. Bowers, "Highly Efficient Vertical Outgassing Channels for Robust, Void-Free, Low-Temperature Direct Wafer Bonding," The 35th Conference on the Physics and Chemistry of Semiconductor Interfaces, Santa Fe, NM, Jan. 2008.
10. J. Vinchant, J. A. Cavaillès, M. Erman, P. Jarry, and M. Renaud, "InP/GaInAsP Guided-Wave Phase Modulators Based on Carrier-induced Effects: Theory and Experiment," *IEEE J. Lightwave Technol.* **10**, 63-70 (1992).

1. Introduction

Recent interest in silicon optical interconnects is driven by the need for high capacity data communication at a relatively low cost. To this end, research on interconnect technology using modulators and switches is being actively pursued. Mach-Zehnder modulators (MZM) using carrier depletion have been reported to have 40 Gb/s operation with 40 V-mm DC drive [1,2]. A ring resonant structure using carrier injection is another approach to implement modulators with compact footprint and narrow optical bandwidth, where speeds up to 12.5 Gb/s were demonstrated with pre-emphasized electrical signals [3]. The tradeoff between modulator efficiency and speed is always an issue for silicon modulators. One new approach to achieve high speed operation while maintaining large modulation efficiency is the hybrid silicon evanescent electroabsorption modulator (EAM) [4], which had 10 dB extinction ratio

(ER), 30 nm optical bandwidth, and over 16 GHz modulation bandwidth. Another new approach is to use carrier depletion inside offset multiple quantum wells (MQW) in a hybrid silicon evanescent MZM. This MZM have less wavelength sensitivity and larger optical bandwidth compared to an EAM. Most importantly, the Mach-Zehnder interferometer (MZI) structure can be made into a 2x2 switch, as demonstrated here, and that can be scaled to larger switches, such as 32x32 nonblocking switches. The MZM was reported with modulation efficiency of 4 V-mm, over 100 nm optical bandwidth, and 28 mW power handling [5], but high speed performance of such a MZM was not demonstrated. In this work, we successfully demonstrated a high speed modulator with 10 Gb/s operation. In addition, by changing the passive waveguide structure of this MZM, a high speed 2x2 switch based on a MZI is implemented and demonstrated on the same platform. Switch arrays are important for interchip and intrachip communication networks, and these elements together with lasers [6], amplifiers, and photodetectors [7], can be integrated as transmitters or receivers for future optical networks.

2. Device description

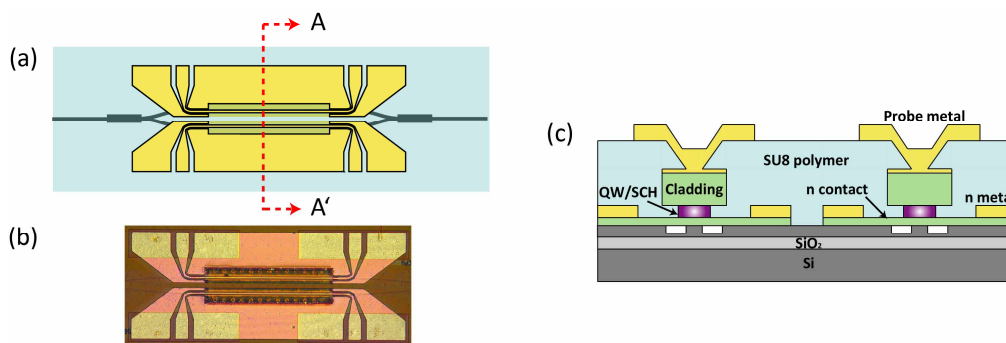


Fig. 1. (a) Top view of a device with a CPW electrode (b) The optical image of the device under microscope (c) Cross section (along A-A') of the hybrid waveguide.

In order to introduce the necessary phase change inside the Mach-Zehnder interferometer for both the hybrid silicon modulator and switch, a III-V epitaxial wafer with doped QW and separate confinement heterostructure (SCH) layer [8] is bonded to patterned silicon waveguides. For such a structure with carriers inside the MQW, the plasma effect dominates at lower reverse bias levels while Pockels, Kerr, and quantum confined Stark effects (QCSE) become more obvious with larger electrical fields. The combination of these effects results in better linearity than devices utilizing simple electro-optic effects.

The top view of a 500 μm MZM is shown in Fig. 1(a). It has two MMIs, each 6 μm wide and 40 μm long, at the input and output functioning as the splitter and the combiner. By changing the 1x2 MMIs to 2x2 MMIs, a switch based on MZI was also fabricated on the same chip. Due to the mode mismatch between the passive and hybrid sections, two 60 μm long tapers, on silicon and III-V section, are added to minimize reflection and increase coupling efficiency. In addition, we use coplanar waveguides (CPW) as the traveling-wave electrode to achieve high speed performance. The optical image of a fabricated device is shown in Fig. 1(b). A thin layer of silicon nitride, which appears as an orange cross region in Fig. 1(b), is deposited at the end of the process to protect the device from scratches. Fig. 1(c) illustrates the cross section of the hybrid section. The device has a 4 μm cladding width while the QW/SCH layers are under-cut to 2 μm to reduce the device capacitance. Moreover, the two arms of the MZM are electrically isolated by etching down the n-contact layer in between. The silicon waveguides have a height of 0.46 μm , a slab height of 0.19 μm , and a width of 0.94 μm .

The devices are fabricated as follows. The III-V epitaxial layers are first bonded to a silicon-on-insulator wafer by using vertical outgassing channel (VOC) technique with an anneal time of 3 hours at 300°C [9]. The substrate is then removed and ready for III-V mesa

fabrication. In order to align contact metal with narrow width of the cladding layer, the cladding mesa is formed by using a self-aligned dry etch process. The sample is then dipped into a mixture of $\text{H}_2\text{O}/\text{H}_2\text{O}_2/\text{H}_3\text{PO}_4$ to create the under-cut in the MQW/SCH layers, while a circular pattern is used as a reference to control the undercut depth. Next, all III-V epitaxial layers are removed on top of passive regions, and a $1\ \mu\text{m}$ n-metal is deposited to form the ground pad of the CPW. A $5\ \mu\text{m}$ thick polymer is then applied to provide additional mechanical support to the thin bonding layer and to separate the probe metal from the bottom n-metal in order to implement the desired CPW design and reduce parasitic capacitances.

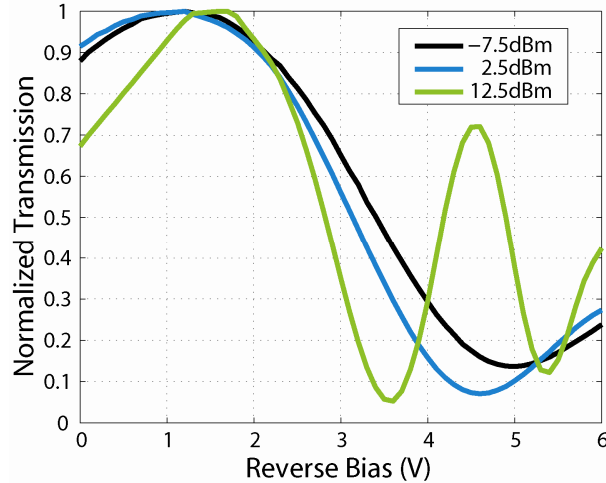


Fig. 2. Modulation efficiency of one port of a silicon hybrid switch with different input power at 1540nm.

3. Device characteristics

The devices were first anti-reflection coated to eliminate the undesired resonance and reduce the reflection on both facets. Two lensed fibers were then used to couple the light in and out of the silicon waveguides. Since there is no difference between modulator and switch inside the hybrid region, the transmission response of the modulator and one port of the switch should be identical. The experiment results of transmission as a function of reverse bias with different input optical powers is shown in Fig. 2. As can be seen, the lowest modulation efficiency is about 2 V-mm, half of the valued reported previously for the same epitaxial structure. The improvement in modulation efficiency is due to the alignment between the III-V crystal facet and waveguide direction such that the Pockels effect adds to the other sources of phase modulation [10].

All three curves in Fig. 2 have a highest transmission at bias other than zero due to fabrication imperfections. As shown in Fig. 2, the voltage-length product decreases from 1.95 V-mm to 1 V-mm as the input power increases from -7.5 dBm to 12.5 dBm. The reduction in voltage-length product can be attributed to the excess carriers generated by two-photon absorption (TPA) at higher optical intensity. Meanwhile, the shift of the peak point to higher reverse bias voltages also indicates the existence of the extra carriers; where stronger electrical field is required to completely deplete the QW/SCH layers. The DC modulation response depends on input optical power level, but the microwave modulation response is unaffected because the frequency range is much higher than the response time of the carriers (carrier life time \sim ns) generated by TPA. To reduce this difference, the bandgap and doping of the QW can be redesigned to decrease the carrier life time such that the contribution of index change from TPA can be reduced.

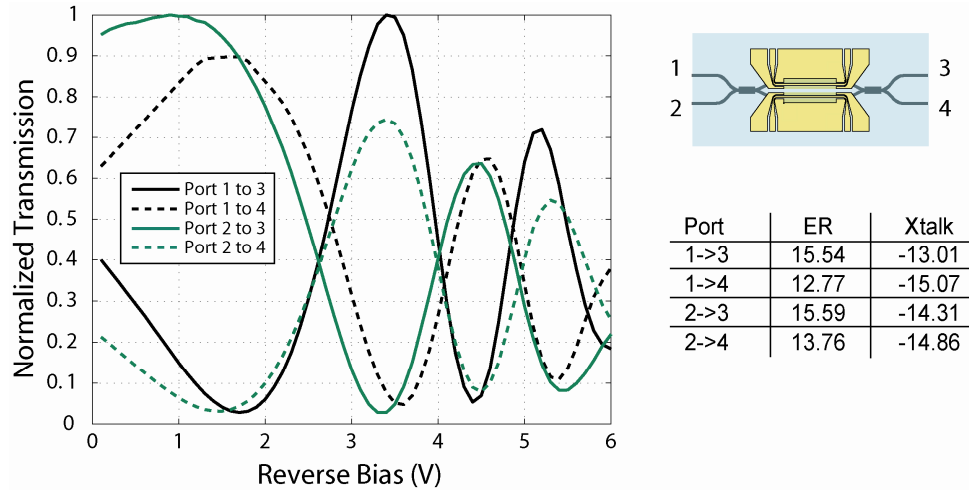


Fig. 3. Transmission of a switch as a function of reverse bias.

The extinction ratios (ER) of MZMs are 12.77 dB, 11.51 dB and 8.64 dB for input powers of 12.5 dBm, 2.5 dBm, and -7.5 dBm, respectively. In addition, the static characteristics of a hybrid silicon switch are also measured as illustrated in Fig. 3. The highest crosstalk is -13 dB and the lowest ER is 12.77 dB for all port configurations. The extinction ratio is limited by QCSE [5], which is more obvious when bias voltage is larger than -3 V. By utilizing the push-pull structure in the future, both arms can be driven and the amplitudes of these two arms are closer so that the destructive interference is closer to zero; and hence increase the ER and decrease the crosstalk.

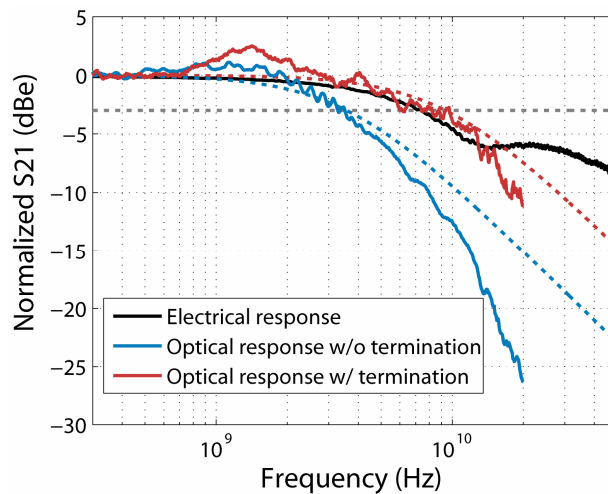


Fig. 4. Experimental electrical and optical response together with RC fitted estimation.

To investigate the high speed performance of the devices, both electrical and optical small signal modulation response were measured using an Agilent 8164A PNA network analyzer and HP 8703A Lightwave component analyzer. As shown in Fig. 4, the electrical response (black curve) depicts a 3 dB cutoff frequency at 7.5 GHz while the optical response without any impedance termination has a 3 dB cutoff frequency at 3.5 GHz (blue curve), which is expected from a lumped RC model simulation (blue dash curve). The degradation of high speed performance is due to the large reflection from the open end of the CPW electrode.

The reflection, however, can be reduced by applying a 25Ω termination such that the cutoff frequency is increased to 8 GHz, sufficient for 10 Gb/s data transmission. The termination used in this experiment has a built-in inductance, hence causing a resonance at 1.5 GHz as illustrated in Fig. 4. A transmission line characteristic impedance of 20Ω and the electrical propagation loss of 5 dB/mm at 10 GHz are calculated by extracting full four-port S parameters.

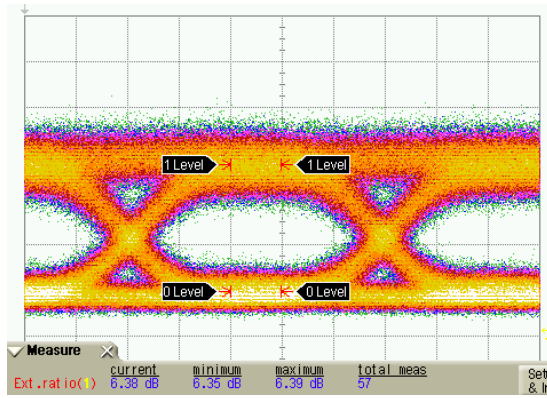


Fig. 5. 10 Gb/s NRZ eye diagram with $2^{31}-1$ PRBS of a MZM at 1550nm.

The MZM was also tested with large signal modulation to characterize its performance for high speed communications. A $2^{31}-1$ pseudorandom bit sequence (PRBS) pattern generator connected to an electrical amplifier is used to provide the drive signal. The device is biased at -3.8 V with 1.5 V swing while the bias at other arm is adjusted to achieve best signal quality. The 10 Gb/s modulated light is then collected by a lensed fiber and amplified with an EDFA following by a filter to eliminate the ASE noise before the signal is sent to an Agilent digital communication analyzer (DCA). The signal has an ER of 6.3 dB, as shown in Fig. 5, which is smaller than the ER (11.6 dB) measured at DC bias due to the partial voltage drop across the series resistance and cladding layer. The eye is clearly open and sufficient for 10 Gb/s operation. The noisy one level is due to the frequency overshoot at 1.4 GHz as mentioned in previous section.

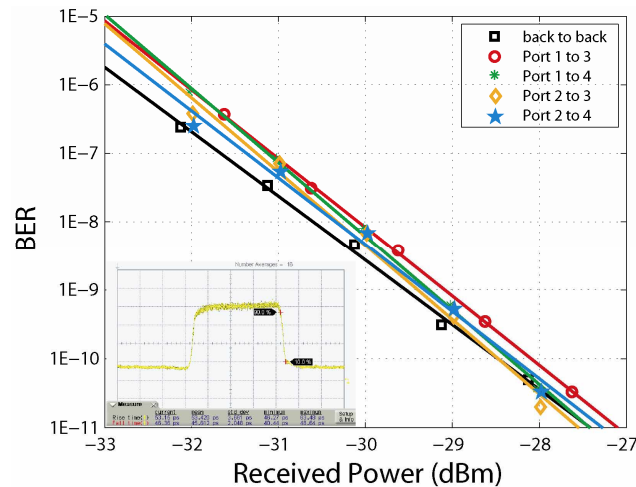


Fig. 6. BER versus optical received power for all ports configurations at 10 Gb/s with $2^{31}-1$ NRZ PRBS. Inset is the response of rise and fall time measured by 10% and 90% with 200ps/div.

A 10 Gb/s bit-error-rate (BER) measurement was also performed to explore the sensitivity at all ports configurations of a switch. As can be seen in Fig. 6, all power penalties are below 0.5 dB at 10^{-9} BER and no error floor is shown. Furthermore, the rise and fall time of the switch is around 50 ps while the drive signal itself has a rise time of around 70 ps as depicted in the inset of Fig. 6. This indicates potential use in a high speed switch or routing network for future high speed optical interconnects.

4. Conclusion

We have demonstrated high speed Mach-Zehnder silicon evanescent modulators and switches utilizing the carrier depletion effect with offset MQWs. The modulator has a $V_{\pi}L$ of 2 V-mm, a modulation bandwidth of 8 GHz, and clear open eye diagram at 10 Gb/s with 6.3 dB ER. The hybrid switch exhibits low power penalty of 0.5 dB for all port configurations at 10 Gb/s data stream format while rise and fall time of 50 ps shows the ability for high speed switching. The hybrid silicon evanescent modulators and switches can be used as interconnects and further integrated with other optical devices to achieve a transparent optical communication system.

Acknowledgments

The authors thank Alex Fang and Di Liang for useful discussions on fabrication and Matt Sysak for the initial idea of using carrier depletion in the modulator. The authors also thank Matt Dummer for helpful suggestions on RF design, John Mack for BER testing and J. Shah for supporting this project. This work is under financial support from DARPA/MTO and ARL.